Converting Adult Pancreatic Islet α Cells into β Cells by Targeting Both Dnmt1 and Arx

Chakravarthy, Harini; Gu, Xueying; Enge, Martin; Dai, Xiaoqing; Wang, Yong; Damond, Nicolas; Downie, Carolina; Liu, Kathy; Wang, Jing; Xing, Yuan; Chera, Simona; Thorel, Fabrizio; Quake, Stephen; Oberholzer, José [**and 3 more**]

How to cite

CHAKRAVARTHY, Harini et al. Converting Adult Pancreatic Islet α Cells into β Cells by Targeting Both Dnmt1 and Arx. In: Cell metabolism, 2017, vol. 25, n° 3, p. 622–634. doi: 10.1016/j.cmet.2017.01.009

This publication URL: https://archive-ouverte.unige.ch//unige:93299
Publication DOI: 10.1016/j.cmet.2017.01.009

AUTHOR QUERY FORM

Journal: CMET

Article Number: 2239

Dear Author,

Please check your proof carefully and mark all corrections at the appropriate place in the proof.

Location in article	Query / Remark: Click on the Q link to find the query's location in text Please insert your reply or correction at the corresponding line in the proof
Q1	Could you please provide the grant number for (1) [H.L. Snyder Foundation], (2) [Swiss National Science Foundation], (3) [HHMI], (4) [Institute of Genetics and Genomics of Geneva], (5) [NIH Beta Cell Biology Consortium (BCBC)], (6) [T32 training award], (7) [Center of Excellence for Stem Cell Genomics], (8) [The Wallenberg Foundation Postdoctoral Scholarship Program], (9) [European Union], (10) [Stanford Child Health Research Institute], (11) [JDRF], (12) [(IMIDIA)], (13) [Stanford University Vice-Provost Undergraduate Education], (14) [Howard Hughes Medical Institute (HHMI)] and (15) [Elser Trust], if any?

Thank you for your assistance.

Article

Cell Metabolism

Converting Adult Pancreatic Islet α Cells into β Cells by Targeting Both *Dnmt1* and *Arx*

Graphical Abstract

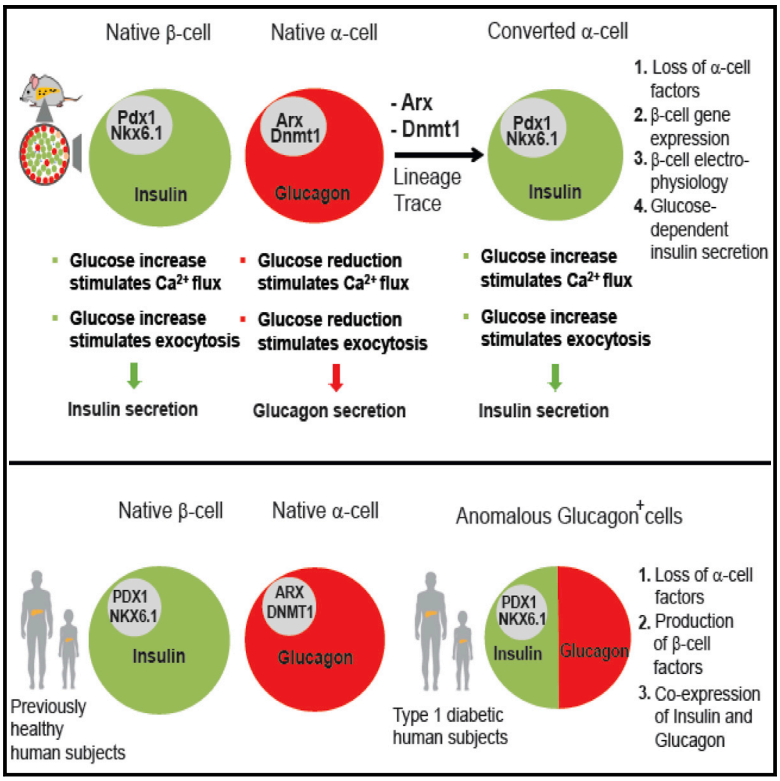

Highlights

- Adult mouse islet α cells convert rapidly into β cells after *Dnmt1* and *Arx* loss
- RNA-seq reveals a strikingly similar gene expression in converted and native β cells
- Converted α cells acquire hallmark functional features of native β cells
- Glucagon$^+$ cells lose DNMT1 and ARX and express β cell markers in human T1D islets

Authors

Harini Chakravarthy, Xueying Gu, Martin Enge, ..., Patrick E. MacDonald, Pedro L. Herrera, Seung K. Kim

Correspondence

seungkim@stanford.edu

In Brief

Chakravarthy et al. dissect the mechanisms maintaining α cell identity and reveal that simultaneous inactivation of the DNA methyltransferase *Dnmt1* and the transcription factor *Arx* in adult mice drives the conversion of α- to β-like cells. In human T1D islets, glucagon+ cells lose DNMT1 and ARX expression and express β cell markers.

Accession Numbers

GSE79457

http://dx.doi.org/10.1016/j.cmet.2017.01.009

CellPress

Please cite this article in press as: Chakravarthy et al., Converting Adult Pancreatic Islet α Cells into β Cells by Targeting Both *Dnmt1* and *Arx*, Cell Metabolism (2017), http://dx.doi.org/10.1016/j.cmet.2017.01.009

Converting Adult Pancreatic Islet α Cells into β Cells by Targeting Both *Dnmt1* and *Arx*

Harini Chakravarthy,[1] Xueying Gu,[1] Martin Enge,[2] Xiaoqing Dai,[3] Yong Wang,[4] Nicolas Damond,[5] Carolina Downie,[1] Kathy Liu,[1] Jing Wang,[1] Yuan Xing,[4] Simona Chera,[6] Fabrizio Thorel,[5] Stephen Quake,[2,7] Jose Oberholzer,[4] Patrick E. MacDonald,[3] Pedro L. Herrera,[5] and Seung K. Kim[1,8,9,*]

[1]Department of Developmental Biology, Stanford University School of Medicine, Stanford, CA 94305, USA
[2]Department of Bioengineering, Stanford University, Stanford, CA 94305, USA
[3]Alberta Diabetes Institute, Department of Pharmacology, University of Alberta, Edmonton, AB T6G2E1, Canada
[4]Department of Surgery/Transplant, University of Illinois, Chicago, IL 60612, USA
[5]Department of Genetic Medicine and Development, Faculty of Medicine, University of Geneva, Geneva 4, Switzerland
[6]Department of Clinical Science, University of Bergen, 5021 Bergen, Norway
[7]Howard Hughes Medical Institute, Stanford, CA 94305, USA
[8]Department of Medicine, Stanford University School of Medicine, Stanford, CA 94305, USA
[9]Lead Contact
*Correspondence: seungkim@stanford.edu
http://dx.doi.org/10.1016/j.cmet.2017.01.009

SUMMARY

Insulin-producing pancreatic β cells in mice can slowly regenerate from glucagon-producing α cells in settings like β cell loss, but the basis of this conversion is unknown. Moreover, it remains unclear if this intra-islet cell conversion is relevant to diseases like type 1 diabetes (T1D). We show that the α cell regulators *Aristaless-related homeobox* (*Arx*) and *DNA methyltransferase 1* (*Dnmt1*) maintain α cell identity in mice. Within 3 months of *Dnmt1* and *Arx* loss, lineage tracing and single-cell RNA sequencing revealed extensive α cell conversion into progeny resembling native β cells. Physiological studies demonstrated that converted α cells acquire hallmark β cell electrophysiology and show glucose-stimulated insulin secretion. In T1D patients, subsets of glucagon-expressing cells show loss of DNMT1 and ARX and produce insulin and other β cell factors, suggesting that DNMT1 and ARX maintain α cell identity in humans. Our work reveals pathways regulated by *Arx* and *Dnmt1* that are sufficient for achieving targeted generation of β cells from adult pancreatic α cells.

INTRODUCTION

Restoration of lost or diseased cells is a focus for intensive efforts in developmental and regenerative biology. Pancreatic islets are a paradigm for investigating organ restoration, reflecting growth in our understanding of the development and maturation by the principal islet cell types (which include insulin $[INS]^+$ β cells, glucagon $[GCG]^+$ α cells, and somatostatin $[SST]^+$ δ cells). Understanding the mechanisms maintaining islet cell fate and function is important for addressing the urgent challenge of restoring islet β cell and α cell function, which is compromised in diseases like type 1 diabetes (T1D). Prior studies have demonstrated that mouse α cells or δ cells can convert into insulin-producing cells following extreme experimental (>99%) β cell ablation; in the case of α cells, about 1% convert toward an insulin-producing fate, without detectable proliferation over a period of 6–7 months (Thorel et al., 2010; Chera et al., 2014). However, the genetic or epigenetic basis of this conversion, including the extent or heterogeneity of reprogramming by individual adult α cells, has not been elucidated. Thus, it remains unknown whether α cell gene targeting in adult mice could enhance conversion into β cells.

Maintenance of fate and function by adult cells likely reflects both genetic and epigenetic mechanisms (Morris and Daley, 2013). Prior studies demonstrate that the transcription factors MAFA, NKX6.1, and PDX1; the proinsulin-processing enzyme PCSK1/3; and, in mice, the glucose transporter encoded by *Slc2a2* are essential regulators of β cell fate and mature function (Arda et al., 2013). By contrast, mouse and human islet α cells require *Aristaless-related homeobox* (*Arx*) to specify α cell fate and maintain production of hallmark factors like glucagon (Collombat et al., 2003, 2007; Kordowich et al., 2011; Papizan et al., 2011; Itoh et al., 2010; Mastracci et al., 2011). Ectopic expression of Pdx1, Nkx6.1, or Pax4 in α cells may be sufficient to induce β cell features in fetal or neonatal α cells (Yang et al., 2011; Collombat et al., 2009; Schaffer et al., 2013).

Surprisingly, studies of *Arx* inactivation in adult mouse glucagon-producing pancreatic cells have not detected clear evidence of direct α to β cell conversion (Courtney et al., 2013; Wilcox et al., 2013). In a prior study of doxycycline (Dox)-induced *Arx* inactivation in mice (Courtney et al., 2013), lineage tracing reflected a schedule of constitutive Dox exposure and did not distinguish ductal cell from α cell progeny. This study concluded that Arx loss in adult mice induced a program of β cell neogenesis resembling embryonic islet development, in which ductal cells expressed the embryonic islet regulator *Neurogenin3* and then *Glucagon* and *Insulin*. In other work, continuous *Arx* inactivation from embryonic stages led to the development of polyhormonal cells (Wilcox et al., 2013). Thus, it remains unclear whether targeted *Arx* inactivation specifically in adult mouse α cells could induce loss of α cell features and acquisition of β cell properties.

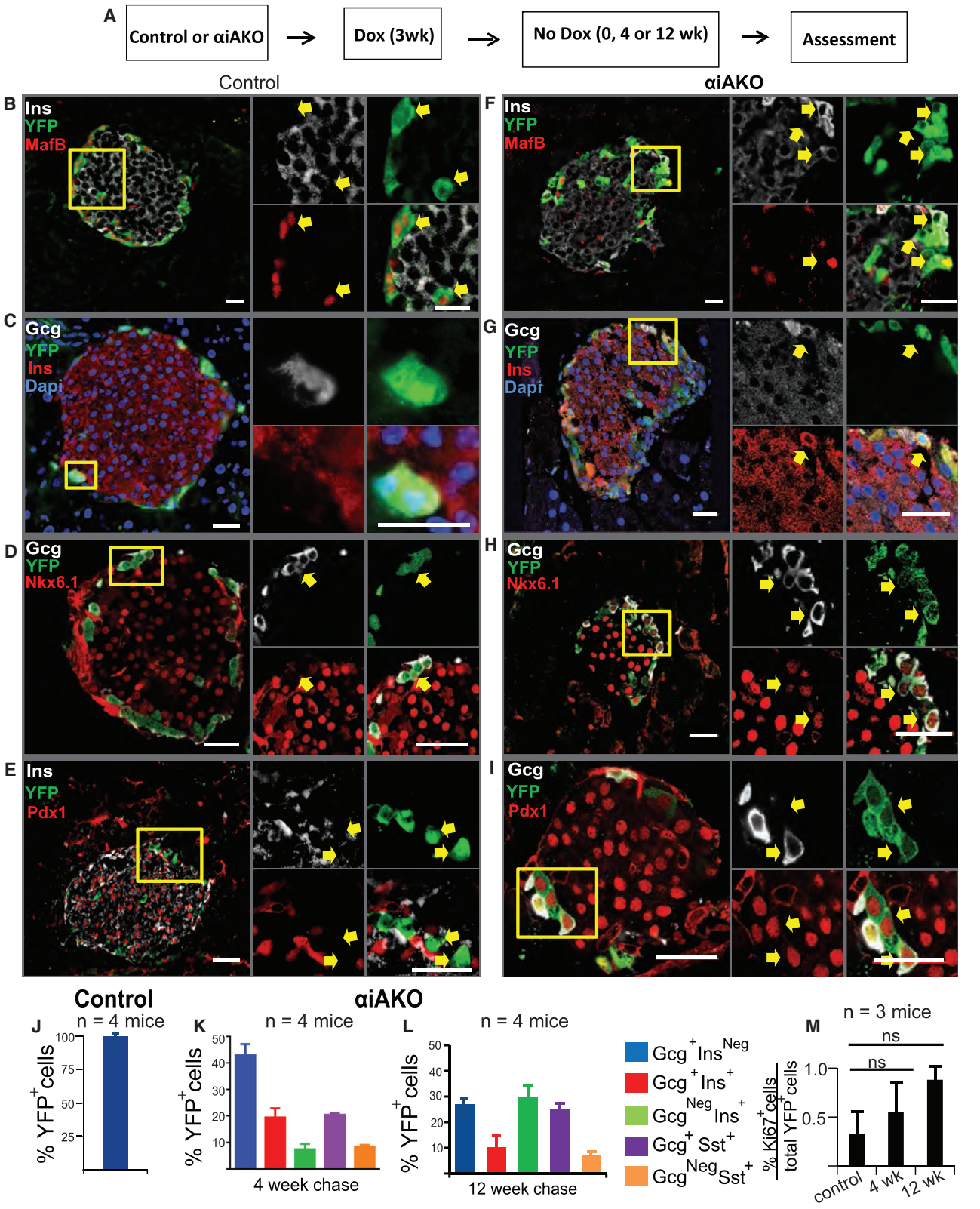

(legend on next page)

In humans with T1D, blunted glucagon output in the setting of severe hypoglycemia is a frequent complication and suggests that islet α cell fate and/or function may be attenuated by disease (Cryer et al., 2003; Pietropaolo, 2013). However, the molecular basis of this α cell dysfunction remains unclear.

Regulation of islet epigenetics by DNA methylation appears to be an important regulatory mechanism during α and β cell differentiation and maturation (Papizan et al., 2011; Avrahami et al., 2015; Dhawan et al., 2011, 2015), and prior studies report an unexpected degree of similarity in gene expression and chromatin modifications of α cells and β cells in mice and humans (Arda et al., 2016; Bramswig et al., 2013; Benitez et al., 2014; Morán et al., 2012). Adult α cells and other islet cells express enzymes like DNA methyltransferase 1 (DNMT1), suggesting a requirement for these factors in maintaining α cell fate (Avrahami et al., 2015; Dhawan et al., 2011; Benitez et al., 2014). Although DNMT1 activity is best understood in the context of maintaining epigenetic "memory" in proliferating cells, recent studies demonstrate DNMT1 function in non-dividing cells (Dhawan et al., 2011). However, direct testing of in vivo DNMT1 requirements in α cells has not been described.

Here, we report that simultaneous inactivation of Arx and Dnmt1 in mouse α cells promotes efficient conversion of α cells into progeny resembling β cells in multiple ways, including insulin production, global gene expression, hallmark electrophysiology, and insulin secretion in response to glucose stimulation. Studies of glucagon$^+$ cells in islets from a subset of humans with T1D similarly reveal loss of *ARX* and *DNMT1*, with a gain of β cell features.

RESULTS

Altered Cell Fates after *Arx* Loss in Adult Mouse α Cells

To determine if *Arx* loss in vivo directly alters adult α cell fate, we developed systems for simultaneous in vivo *Arx* inactivation and lineage tracing in mouse α cells (Experimental Procedures; Figure S1A, available online). We used previously described mice (Thorel et al., 2010) harboring a doxycycline-inducible *Gcg*-driven *reverse tet transactivator* (*Gcg-rtTA)* to direct Cre recombinase expression from a *Tet-O-Cre* transgene in Gcg$^+$ α cells. Cre then activates lineage-independent *YFP* transgene expression from the *Rosa26* locus. Intercrosses generated α cell-inducible Arx knockout (αiAKO) mice (Figure S1A) harboring a Cre-recombinase-sensitive floxed *Arx* allele (Fulp et al., 2008) and the three alleles described above. Briefly, in αiAKO islets, Dox exposure should stimulate Cre recombinase expression specifically in Gcg$^+$ α cells. Cre then inactivates the floxed *Arx* allele and activates *YFP* transgene expression from the *Rosa26* locus.

Over 90% of Gcg$^+$ cells were labeled with yellow fluorescent protein (YFP) in 2-month-old control *Gcg-rtTA, Tet-O-Cre, Rosa26-YFP* animals exposed to Dox for 3 weeks or αiAKO animals exposed to Dox for 3 weeks, followed by a 4- or 12-week "chase" period without Dox (Figure 1A). We have previously found extremely low (0.1%–0.2%) non-specific labeling of YFP+ cells in control mice when doxycycline is given after birth (Thorel et al., 2010). Loss of Arx protein in αiAKO mouse α cells was confirmed by immunostaining (Figures S1B and S1C). We did not detect differences in glycemia during ad libitum feeding or after overnight fasting in control and αiAKO mice (Table S4). After 0, 4, or 12 weeks without Dox, we sacrificed mice and immunostained the pancreas to assess islet cell fates. By 4 weeks, 50% of YFP$^+$ cells without Arx showed evidence of failure to maintain α cell identity. This included loss of α cell gene products like glucagon or MafB (Figures 1F, 1I, 1K, and S2F–S2T). Notably, the majority of cells (60%) co-expressing glucagon or MafB also produced gene products not observed in normal α cells, like insulin, Pdx1, or Nkx6.1 (Figures 1F–1I and S2); somatostatin; and, rarely, ghrelin or pancreatic polypeptide (Figures 1K, S3A–S3C, and S3E–S3G). Quantification of YFP$^+$ cell phenotypes revealed that 20% co-expressed α cell (Gcg and MafB) and β cell gene products (Ins, Pdx1, and Nkx6.1; Figures 1G–1I, 1K, S2I, and S2J). Only 6% of YFP$^+$ cells produced insulin without glucagon. After 12 weeks off Dox, this population of YFP$^+$ Ins$^+$ Gcg^{Neg} cells increased to 29% of YFP$^+$ cells, but none expressed the mature β cell marker MafA (Figures S3D and S3H). By contrast, YFP$^+$ cells remained 99.8% Gcg$^+$ Ins^{Neg} in control mice (Figures 1C and 1J). In control and αiAKO mice, we scored production of the proliferation marker Ki67 and did not detect changes of YFP$^+$ cell proliferation after 4 and 12 weeks off Dox (Figure 1J; Table S2). However, this does not exclude the possibility that α cell proliferation occurred at earlier times after *Arx* deletion. We also did not detect induction of *Neurogenin3* (*Neurog3*), which encodes a bHLH transcription factor expressed in fetal pancreatic endocrine progenitor cells (Gradwohl et al., 2000; Gu et al., 2002). Thus, loss of *Arx* led to failure of adult mouse α cells to maintain their differentiated fates, leading to time-dependent adoption of alternate islet cell fates, mainly a population of polyhormonal cells, and a smaller fraction resembling islet β, δ, ε, and pancreatic polypeptide (PP) cells. These findings and approaches differ from those reported by Courtney et al., 2013, who constitutively inactivated *Arx* in adult Gcg$^+$ cells and observed islet hyperplasia, with a large increase in the Ins$^+$ Gcg^{Neg} cell number accompanied by reactivation of *Neurog3* and without durable increases of polyhormonal Gcg$^+$ cells expressing Sst, ghrelin, or PP (see Discussion).

Figure 1. Loss of α Cell Identity after Deletion of Arx

(A) Schematic showing experimental design for Dox treatment of knockout and control animals.

(B–I) Immunostaining showing expression of α and β cell markers (B and F) MafB, (B, C, and E–G) Ins, (C, D, and G–I) Gcg, (D and H) Nkx6.1, and (E and I) Pdx1, with YFP in control and αiAKO mice 4 weeks after Dox treatment. Yellow boxes show the specific area of the islet, which is enlarged and represented by arrows on the right to demonstrate gene expression within specific cells or sets of cells. Scale bars, 25 μm.

(J–L) Quantification of α to β cell conversion in control mice at the end of 3 weeks of Dox treatment (time 0) (J) and αiAKO mice at the end of a 4-week chase and 12-week chase (K and L).

(M) Quantification of Ki67$^+$ YFP$^+$ cells at the end of a 4-week chase and 12-week chase compared to controls (N = 3 mice). Bar graph data are represented as mean ± SD. N = 4 mice per time point.

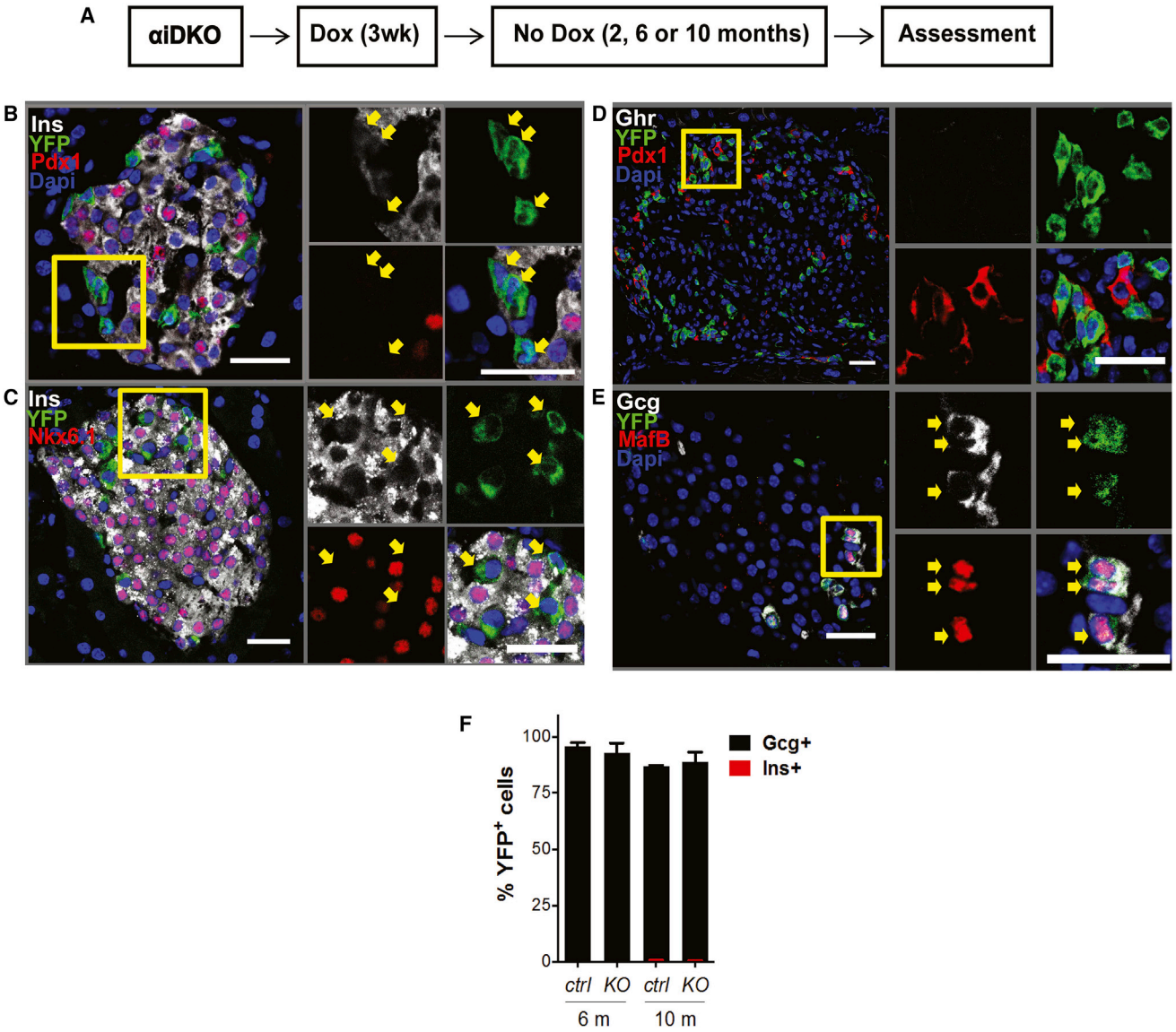

Figure 2. α Cells Maintain Their Fate in the Absence of Dnmt1

(A) Schematic showing experimental design for Dox treatment of knockout and control animals.

(B–E) Immunostaining showing expression of α, β, δ, and ε cell markers (E) Gcg, (E) MafB, (B and C) Ins, (B and D) Pdx1, (C) Nkx6.1, and (D) ghrelin with YFP in αiDKO mice 10 months after Dox treatment. Yellow boxes show the specific area of the islet, which is enlarged and represented by arrows on the right to demonstrate gene expression within specific cells or sets of cells. Scale bars, 25 μm.

(F) Percentage of YFP^+ cells that express glucagon or insulin in knockout and control mice. Bar graph data are represented as mean ± SD. N = 4 mice per time point.

α Cell Identity Is Unaltered by Loss of Endogenous *Dnmt1*

Our finding that over 60% of α cells failed to express insulin after *Arx* loss suggested that α cell fate was likely maintained by additional regulatory factors. *Dnmt1* is an enzyme that functions to regulate genome-wide gene expression by methylating cytosine residues within regulatory regions of genes. Others have reported that *Dnmt1* is important for islet cell fate maintenance across species (Dhawan et al., 2011, 2015; Bramswig et al., 2013; Anderson et al., 2009). Thus, we postulated that removal of *Dnmt1* might compromise α cell fate. To test this, we constructed mice harboring the alleles *Gcg-rtTA*, *Tet-O-Cre*, $Dnmt1^{f/f}$, and *Rosa26-YFP* ("αiDKO mice"; Figure 2A). After Dox exposure, we detected loss of Dnmt1 in YFP^+ cells; however, YFP^+ cells produced no detectable insulin, Pdx1, or Nkx6.1, even 10 months after DOX removal (Figures 2B and 2C). Instead, YFP^+ cells maintained expression of glucagon and MafB and did not produce detectable Sst or Ghr (Figures 2D–2F). Thus, unlike targeted *Arx* loss in α cells, targeted *Dnmt1* inactivation did not discernably alter α cell fate.

α Cells with Combined *Arx* and *Dnmt1* Loss Resemble β Cells

To test whether simultaneous loss of Arx and Dnmt1 might alter the pattern of α cell conversion in adult mice, we intercrossed mice to produce progeny permitting Dox-dependent α cell inactivation of *Dnmt1* and *Arx* combined with Rosa26-YFP lineage tracing (Experimental Procedures; Figure S1A). Mice with the six alleles *Gcg-rtTA*, *Tet-O-Cre*, *Arx*$^{f/Y}$, *Dnmt1*$^{f/f}$, and Rosa26-*YFP* (hereafter, "αiADKO mice") and controls were exposed to Dox for 3 weeks, followed by 4 or 12 weeks without Dox (Figure 3A). Loss of Arx or Dnmt1 in α cells, labeled with over 90% efficiency by YFP, was confirmed by immunostaining (Figures S1B–S1E and S4U–S4Y).

After 4 weeks, immunostaining revealed that 50% of YFP$^+$ cells failed to maintain α cell identity, showing either loss of α cell products like glucagon and MafB or co-expression of glucagon and MafB with gene products characteristic of β cells like insulin, Nkx6.1, and Pdx1 (Figures 3B–3D, 3G, 3I, and S4A–S4T) or δ cells (Sst; Figures 3F and 3J). At 4 weeks, 23% of YFP$^+$ cells in αiADKO mice co-expressed α and β cell gene products like glucagon and insulin, and 16% expressed β cell gene products like Pdx1 and insulin without detectable glucagon or MafB (Figures 3J and S4A–S4T). Only 14% of YFP$^+$ cells produced Sst (Figure 3J). By contrast, we did not detect production of PP or ghrelin in YFP$^+$ cells. After 12 weeks, immunostaining revealed that 82% of αiADKO YFP$^+$ cells had lost their α cell fate. In total, 50% of YFP$^+$ cells had lost the expression of either Gcg or MafB or both and produced β cell factors, including insulin, Pdx1, and Nkx6.1 (Figures 3B–3G, 3K, and S4A–S4T). Like in αiAKO mice, we did not detect changes in Ki67 or Neurog3 in αiADKO mice (Figures 3L and S4Z).

By 12 weeks, we also observed some YFP$^+$ Ins$^+$ Gcg^{Neg} cells expressing the glucose transporter Slc2a2 and MafA, markers and regulators of native β cells (Figures 3H and 3I). A total of 27% of YFP$^+$ cells in αiADKO mice produced Sst (Figures 3F and 3K), and 10% co-expressed Gcg and insulin (Figure 3K). Thus, using lineage tracing and conditional genetics to inactivate *Arx* and *Dnmt1*, we observed evidence of extensive direct α cell conversion into progeny resembling β cells.

Single-Cell RNA-Seq Reveals That Converted α Cells Closely Resemble Native β Cells

To investigate further the extent of α cell conversion toward fates resembling β cells, we performed single-cell RNA sequencing (scRNA-seq) after purifying YFP$^+$ cells and control (YFP^{Neg}) cells from αiADKO mice and control mice by fluorescent-activated cell sorting (FACS). After Dox exposure, we obtained 127 YFP$^+$ cells at 8 weeks ("early"; light gray bars, Figure 4A) and 44 YFP$^+$ cells at 12 weeks ("late"; dark gray bars, Figure 4A), in addition to YFP^{Neg} control native β cells, α cells, or δ cells (black bars, Figure 4A). All YFP$^+$ cells expressed the *YFP* transgene and pan-endocrine genes like chromogranin A (CHGA) and chromogranin B, demonstrating the islet endocrine origin of these cells. These did not express endocrine precursor markers such as *Ngn3* mRNA (Figure 4A), similar to prior findings with α cell conversion after β cell ablation (Thorel et al., 2010; Chera et al., 2014). Consistent with our immunohistological analysis, YFP$^+$ cells from both early and late collections clustered into three major populations after t-distributed stochastic neighbor embedding (tSNE) dimensionality-reduction analysis: (1) cells that are similar to normal α cells, (2) cells that are similar to normal β cells, and (3) cells that express other islet hormones such as Sst (Figure 4B; data not shown).

Approximately 20% of the YFP$^+$ cells at 8 weeks exclusively express insulin and other β cell genes. The majority of the YFP$^+$ cells from this time point maintained mRNA expression of the α cell gene *MafB* (Figure 4A). In addition to these distinct populations, YFP$^+$ cells that exhibit features of two or more islet cell types (including polyhormonal mRNA expression) occurred more frequently at 8 weeks than at later times. At 12 weeks, RNA-seq revealed that nearly 80% of the YFP$^+$ cells expressed *Ins1* and *Ins2*, and the majority of these did not express mRNAs encoding other islet hormones. Moreover, just 7% of YFP$^+$ cells exclusively expressed Gcg at 12 weeks. Thus, α cells in αiADKO mice appeared to preferentially convert toward β cell fates. Ingenuity Pathway Analysis (IPA) of these datasets identified pathways in converted α cells that are crucial for β cell identity and function, including maturity onset diabetes of the young (MODY) signaling factors (Hnf1a, Pdx1, and Gck) (Figures 4C and 4D). RNA-seq confirmed that a subset of the converted α cells expressed many of these regulators (like Pdx1, Nkx6.1, and Glis3) and their known downstream targets, such as Scn9a, Gck, and Slc2a2, which are established effectors of β cell function (Figure 4E). Together, scRNA-seq and our analysis provide unprecedented genome-scale evidence for the range, trajectory, and extent of gene expression changes in α cells directly converting toward β cells after conditional *Arx* and *Dnmt1* inactivation.

Electrophysiological Resemblance of Converted α Cells and Native β Cells

In electrophysiological studies, mouse α and β cells have long been distinguished by characteristic differences in the voltage-dependent inactivation of Na^+ channels (Göpel et al., 2000) and, more recently, by opposing glucose-dependent exocytotic responses to serial membrane depolarization (Ferdaoussi et al., 2015; Dai et al., 2014). Our scRNA-seq studies reveal upregulation of genes mediating the β cell Na^+ current (*Scn9a*) and contributing to β cell glucose sensing (*Slc2a2*) in the converted α cells, but not in the unconverted α cells from αiADKO mice (Figure 4E). We postulated that converted α cells lose the electrophysiological response features of α cells and acquire β cell responses. To assess this, we dispersed islets into single cells from αiADKO mice after 12 weeks of Dox treatment and measured Na^+ inactivation and glucose-dependent capacitance responses in YFP$^+$ cells. We find that Na^+ current inactivation is half maximal at −46 and −96 mV in α and β cells, respectively, from control mice (n = 13 and 9 cells; Figure 5A). Non-converted α cells from the αiADKO mice (Ins^{Neg},YFP$^+$) maintained their right-shifted Na^+ current inactivation, which was half-maximal at −49 mV (n = 21 cells; Figure 5B). However, Na^+ current inactivation in converted α cells from the αiADKO mice (Ins$^+$,YFP$^+$), resembled that of native β cells, in which most channels (~70%) inactivated half-maximally at −94.2 mV (n = 27 cells; Figure 5B).

Glucose stimulation amplifies the exocytotic response to membrane depolarization in β cells (Ferdaoussi et al., 2015) but suppresses the response in α cells (Dai et al., 2014).

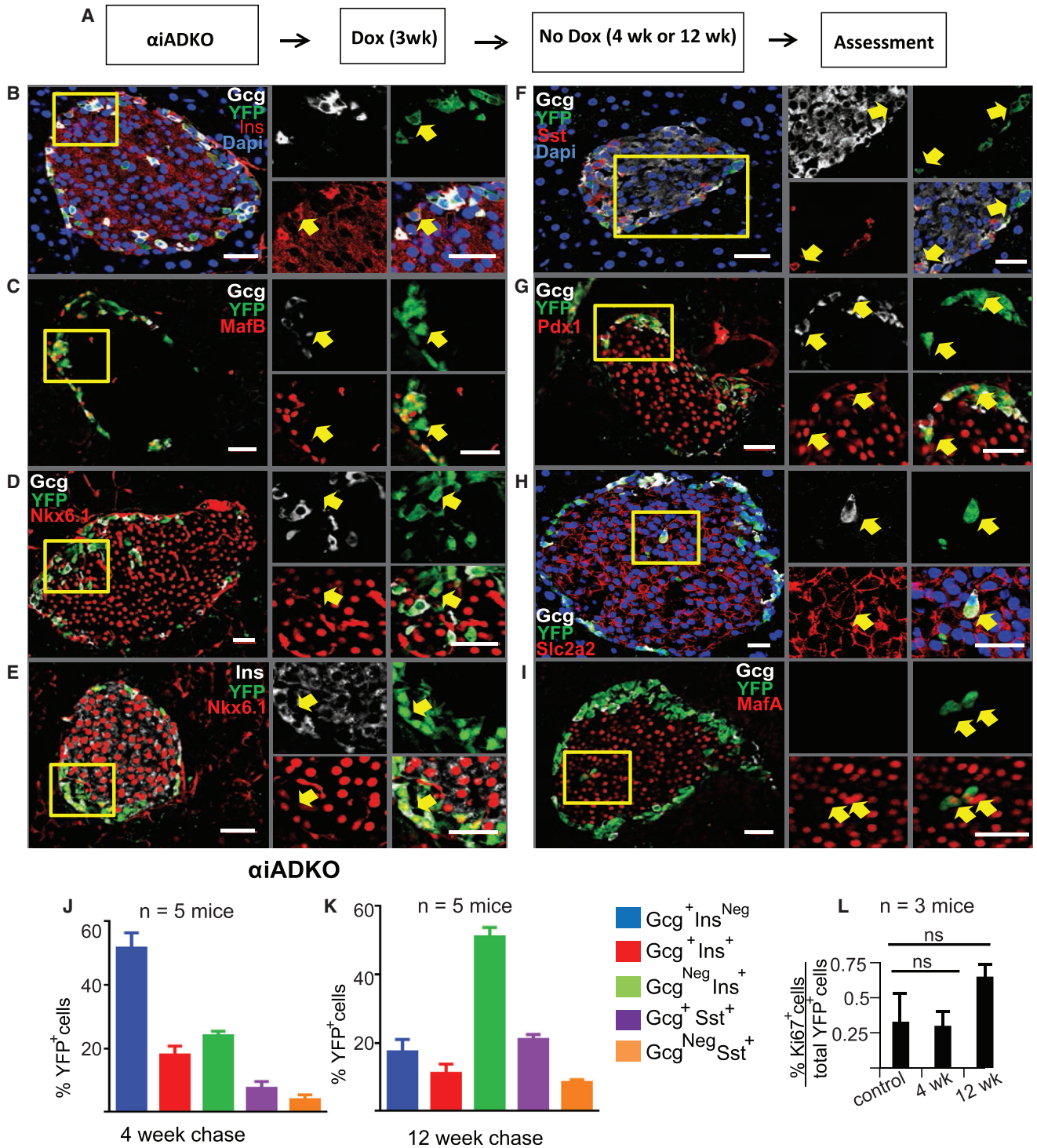

Figure 3. Expression of β Cell Genes in Murine α Cells Lacking Dnmt1 and Arx

(A) Schematic showing experimental design for Dox treatment of knockout and control animals.

(B–I) Immunostaining showing expression of α, β, and δ cell markers (B and E) Ins, (B–D and F–I) Gcg, (C) MafB, (D and E) Nkx6.1, (F) Sst, (G) Pdx1, (H) Slc2a2, and (I) MafA with YFP in αiADKO mice 12 weeks after Dox treatment. Yellow boxes show the specific area of the islet, which is enlarged and represented by arrows on the right to demonstrate gene expression within specific cells or sets of cells. Scale bars, 25 μm.

(J and K) Quantification of α to β cell conversion in αiADKO mice at the end of a (J) 4-week chase and (K) 12-week chase.

(L) Quantification of Ki67$^+$ YFP$^+$ cells at the end of a 4-week chase and 12-week chase compared to controls (N = 3 mice). Bar graph data are represented as mean ± SD. N = 4 mice per time point.

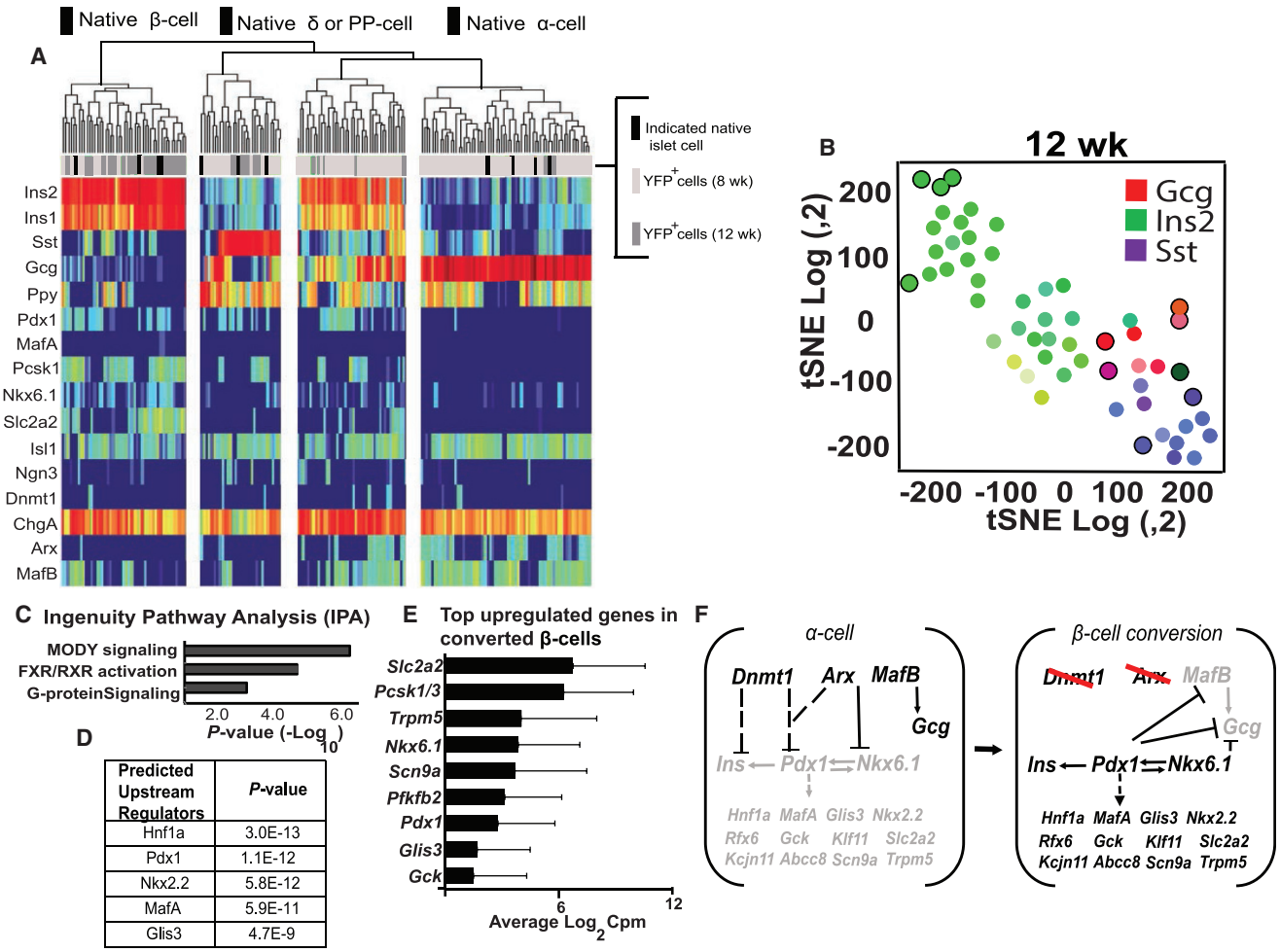

Figure 4. scRNA-Seq Analysis of Mouse α cells Undergoing Loss of Identity

(A) Heat map generated from single cells obtained from two αiADKO mice 8 and 12 weeks after Dnmt1 and Arx deletion (N = 2 mice). Black bars represent normal islet cells, and light gray and dark gray bars represent individual YFP$^+$ cells obtained from αiADKO mice at the 8-week and 12-week time points, respectively.

(B) tSNE plot generated from single cells obtained from αiADKO mice 12 weeks after Dnmt1 and Arx deletion. Black circles represent normal islet cells. Green circles represent individual YFP$^+$ cells obtained from αiADKO mice. The color inside each circle indicates whether the cell expressed Gcg (red), Ins (green), or Sst (purple). Intermediate colors represent intermediate cell states.

(C and D) Key predicted pathways (C) and gene regulators (D) generated by IPA comparing single cells obtained from αiADKO mice 8 weeks and 12 weeks after Dnmt1 and Arx deletion and progressing from an α cell state to a β cell state.

(E) Top upregulated genes in converted α cells represented as the average of $\log_2$ counts per million (Cpm) values from single cells expressing insulin alone obtained from αiADKO mice at the 12-week time point. The average insulin expression in these cells is 16.1 (±0.37) cpm.

(F) A model for activation of a β cell gene regulatory network in cells undergoing α to β cell conversion. Dashed lines and arrows represent indirect transcriptional relationships between regulators and targets. Solid lines and arrows represent established direct transcriptional relationships between regulators and targets. Repressed genes are in gray font, whereas induced genes are in black font.

Accordingly, exocytosis in α cells from the control mice is suppressed by a rise in glucose (n = 16 cells) and amplified by a drop in glucose (n = 21; Figures 5C and 5D), and this is also observed in the non-converted (Ins^{Neg},YFP$^+$) α cells from the αiADKO mice (n = 24 and 13 cells; Figures 5E and 5F). The converted α cells (Ins$^+$,YFP$^+$) from the αiADKO mice, however, again resembled native β cells, in which the exocytotic response was suppressed by a drop in glucose (from 20 to 2 mM; n = 14 cells) and amplified by a rise in glucose (from 2 to 20 mM; n = 23 cells; Figures 5G–5J). Together, these studies reveal a striking functional switch from α cell to β cell phenotypes in converted mouse β cells after conditional deletion of *Dnmt1* and *Arx*.

Glucose-Dependent Insulin Secretion by Converted α Cells and Native β Cells

Our electrophysiological studies and findings suggested that converted α cells might also functionally resemble native β cells by (1) increasing their intracellular calcium ($[Ca^{2+}]_i$) upon glucose stimulation and (2) secreting insulin in response to glucose, two tightly coupled functions. To assess this, we dispersed islets into single cells from control (see Experimental Procedures) and αiADKO mice after Dox treatment, FACS purified the YFP$^+$ cells, and then measured calcium influx and insulin secretion kinetics in response to glucose by relevant FACS-purified cells using a microfluidics perifusion system

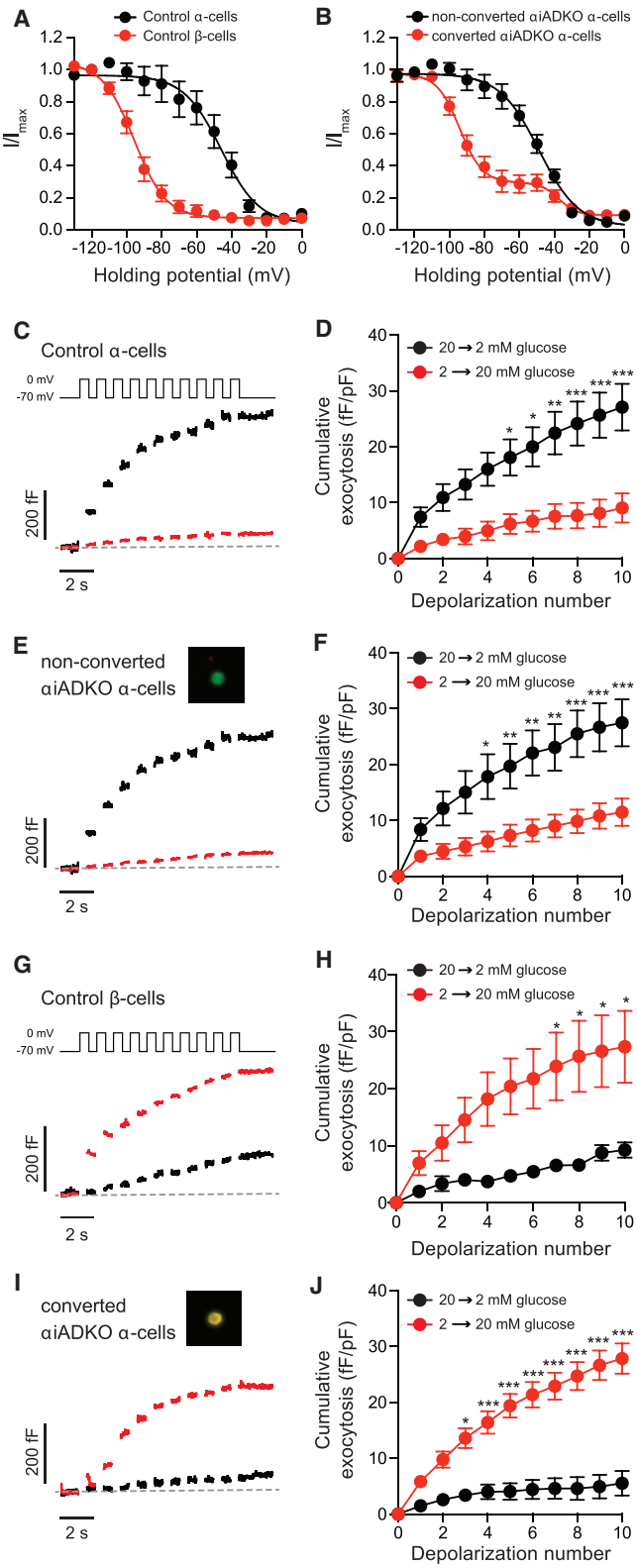

Figure 5. Electrophysiological Properties of Converted α Cells

(A) Voltage-dependent inactivation of Na^+ channels is left shifted in control β cells (red; n = 9) compared with control α cells (black; n = 13). Total mice = 3.

(B) Inactivation of Na^+ currents in non-converted (Ins^{Neg},YFP^+) αiADKO α cells (black; n = 21, mice = 3) was identical to that of the control α cells, whereas the majority (~70%) of Na^+ current inactivation in the converted (Ins^+,YFP^+) αiADKO β cells (red; n = 27, mice = 3) was left shifted similarly to that observed in β cells.

(C–J) Single-cell exocytosis was measured by monitoring capacitance increases in response to a series of membrane depolarizations following transition from 20 to 2 mM glucose (black) or 2 to 20 mM glucose (red). Representative traces (C, E, and G) and averaged data (D, F, and H) are shown. In control α cells (C and D), exocytosis was amplified by lowering glucose (n = 21, mice = 2) and suppressed by raising glucose (n = 16, mice = 2). Identical results were observed (E and F) in non-converted (Ins^{Neg},YFP^+; inset) αiADKO α cells (n = 13 and 24, mice = 3). In control β cells (G and H), the exocytotic response was amplified by raising glucose (n = 8) and suppressed by lowering glucose (n = 6, mice = 2). In converted (I and J; Ins^+,YFP^+; inset) αiADKO α cells, however, the response was reversed to recapitulate a β cell phenotype, such that raising glucose amplified the exocytotic response (n = 23, mice = 3), whereas lowering glucose suppressed it (n = 14). *p < 0.05; **p < 0.01; ***p > 0.001.

(Adewola et al., 2010: Xing et al., 2016). As expected, GFP^+ β cells from mouse insulin promoter-GFP (MIP-GFP) mice secreted insulin, but not glucagon, in response to glucose stimulation, and $Venus^+$ cells from glucagon-Venus mice secreted glucagon when challenged by glucose reduction (Figures 6A, 6B, S5A, and S5B). By contrast, converted α cells from αiADKO mice secreted insulin in response to high glucose (Figure 6C). Compared to native β cells, the level of insulin secretion by converted αiADKO α cells was lower but prolonged after glucose challenge (Figures 6A and 6C). Glucagon secretion by pooled YFP^+ αiADKO α cells and $Venus^+$ control α cells from glucagon-Venus mice was similar (Figure S5C), consistent with our finding that a subset of DOX-exposed αiADKO α cells maintain glucagon expression and electrophysiological features of native α cells.

Glucose-stimulated insulin secretion in native β cells is tightly coupled to glucose metabolism, membrane depolarization, and transient intracellular increases of $[Ca^{2+}]_i$. We assessed $[Ca^{2+}]_i$ changes in isolated control α and β cells and in YFP^+ αiADKO cells during exposure to basal (2.8 mM) and high (14 mM) glucose concentrations or to potassium chloride (KCl), a general membrane depolarizer. Single-cell calcium imaging revealed that KCl provoked increased $[Ca^{2+}]_i$ in β cells from MIP-GFP mice, α cells from glucagon-Venus mice, and YFP^+ cells from αiADKO mice (Figures 6D–6F). After exposure to 14 mM glucose, we observe an average increase of $[Ca^{2+}]_i$ in native β cells and YFP^+ αiADKO cells, but not in native α cells (Figures 6D–6F, dark gray bars). Together, our physiological studies revealed that converted mouse α cells acquired multiple cardinal functional features of normal β cells, supporting our molecular findings.

Evidence of Altered $Glucagon^+$ Cell Fates in Pancreas from T1D Subjects

Impaired glucagon responses to hypoglycemia in T1D (Cryer et al., 2003; Pietropaolo, 2013) have suggested that islet α cell fates may be altered in T1D. To determine whether changes, including loss of islet DNMT1 and ARX, might occur in human T1D, we used immunohistochemistry to analyze cell-enriched transcription factor and hormone expression in pancreata from control (Figures S6A–S6F) and T1D donors

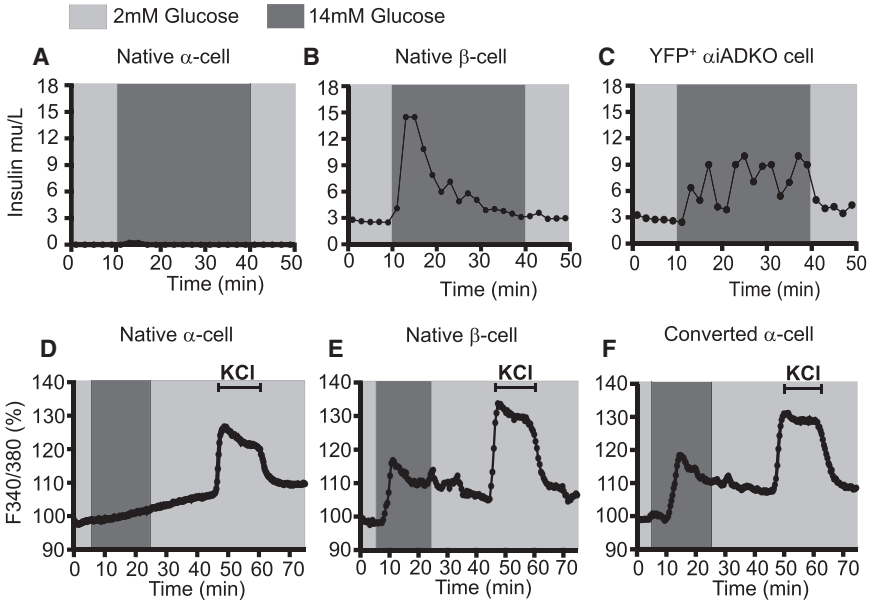

Figure 6. Insulin Secretion and Calcium Signaling Properties of Converted α Cells

(A–C) Temporal insulin secretion profiles of 5,000 YFP$^+$ cells from glucagon-Venus mice (N = 3 mice) (A), MIP-GFP mice (N = 3 mice) (B), and αiADKO mice (N = 4 mice) (C) perfused with basal (2 mM glucose) and stimulatory (14 mM glucose) solutions at the indicated time points.

(D–F) Intracellular calcium profiles indicated by Fura-2 ratio of the fluorescence intensities (340/380 nm) of Venus$^+$ cells and GFP$^+$ from glucagon-Venus mice (N = 3 mice) (D), MIP-GFP mice (N = 3 mice) (E), and αiADKO mice (N = 5 mice) (F) perfused with basal (2 mM glucose) and stimulatory (14 mM glucose or 30 mM KCl) solutions at the indicated time points.

In (A)–(F), cells are FACS purified from the indicated mice.

(Figures S6G–S6M). As expected, previously healthy control subjects aged 4, 7, and 26 years (Table 1) produced INS, PDX1, and NKX6.1 exclusively in β cells; GCG and ARX in α cells; and SST in δ cells (Figures S6A–S6E). DNMT1 (Figure S6F) was expressed in a subset of α and β cells (Figure S6E). There was no detectable co-expression in controls of insulin with glucagon, Sst, or ARX or glucagon with PDX1 or NKX6.1 (Figures S6A–S6E; quantification in Figures S6N–S6R). In samples from donors with T1D for 4, 5, 7, 23, or 33 years (Figures S6G–S6M and S7B–S7L), we observed a pronounced loss of INS$^+$ cells. However, the expression of a variety of pan-endocrine markers, including PAX6, NKX2.2, and CHGA, was maintained in hormone$^+$ cells (H.C. and S.K., unpublished data).

In T1D islets from donors with 4–5 year disease duration, we detected additional abnormal GCG$^+$ cells: 10% of remaining GCG$^+$ cells lacked ARX or produced characteristic β cell factors like PDX1 or NKX6.1 (Figures S6G, S6I, S6J, S6N, S6P, S6Q, S7B, S7C, and S7F). Moreover, bi-hormonal GCG$^+$ INS$^+$ cells were also observed in 2% of islets from donors with T1D for 4 or 5 years (Figure S6H, S6O, and S7D), which correlated with loss of DNMT1 in these cells (Figure S6M, yellow and white arrows; Figure S6S). In samples from subjects with longer T1D duration, approximately 5% of remaining GCG$^+$ cells lacked ARX or co-expressed NKX6.1. However, GCG$^+$ PDX1$^+$ or bihormonal GCG$^+$ INS$^+$ cells were not detected in these samples (Figures S7A–S7C and S7F). Thus, our studies of T1D islets from five donors revealed (1) loss of the hallmark α cell features and gain of the β cell features in a fraction of GCG$^+$ cells and (2) GCG$^+$ INS$^+$ expression in cells lacking ARX and DNMT1.

DISCUSSION

Dissecting and controlling the mechanisms governing cell fate is a central challenge for developmental and regenerative biology (Kim et al., 2016). We investigated α cells in mice affording conditional genetics, lineage-tracing, scRNA-seq, and functional analyses and in humans with T1D and β cell destruction. To determine the genetic mechanism by which insulin-producing cells might be spontaneously regenerated from α cells, we inactivated two genes, *Arx* and *Dnmt1*, in adult pancreatic α cells and found this was sufficient for direct, efficient conversion of islet α cells into progeny resembling β cells. We investigated islet cell identity in the human T1D pancreas and discovered changes of multiple regulators in glucagon$^+$ islet cells, including loss of ARX and DNMT1. We speculate that such changes could underlie α cell dysfunction in T1D.

Directing effective conversion of non-β cells into insulin-producing cells could be crucial for achieving regenerative goals. Studies here revealed efficient formation of insulin-expressing cells within 3 months by 50%–80% of α cells after targeted inactivation of *Arx* and *Dnmt1*. Converted α cells resembled native β cells in their electrophysiology and ability to secrete insulin in response to glucose stimulation. Thus, our histology, lineage-tracing, scRNA-seq analysis, electrophysiological, and hormone studies provided an unprecedented assessment of the trajectory of cells undergoing α to β cell conversion. Formation of insulin-producing cells after targeted inactivation of *Arx* alone produced fewer glucagon^{Neg} insulin$^+$ cells and more polyhormonal cell types, whereas *Dnmt1* inactivation alone was insufficient to induce insulin$^+$ α cells.

Prior studies postulated that effective somatic cell conversion may require at least two steps of re-programming: a "priming" step to poise genes for alternative expression and loss (or gain) of a cell-type-specific "master" regulator (Efe et al., 2011; Shu et al., 2013). The modest or ineffective α cell conversion following Dnmt1 loss alone or Arx loss alone is consistent with this hypothesis. We speculate that Dnmt1 loss could constitute a priming step, whereas loss of Arx, a master regulator of α cell fate, is a required concurrent step to achieve α to β cell conversion. The mechanisms by which deletion of Dnmt1 contributes to loss of α cell identity are not known. However, it seems likely that the reduction in promoter/enhancer methylation within transcriptional control sequences of key β cell genes, such as *Insulin*, *Pdx1*, and *Nkx6.1* (Avrahami et al., 2015., Akinci et al., 2012; Park et al., 2008), combined with loss of Arx, permits activation of these genes (Papizan et al., 2011).

Table 1. List of Human Pancreas Samples

Age	Sex	Disease	Disease Duration	Number of Insulin$^+$ Cells Scored
27	male	normal	not applicable	not applicable
7	male	normal	not applicable	not applicable
4	male	normal	not applicable	not applicable
9	female	T1D	5	19
8	female	T1D	4	11
22	male	T1D	7	122
32	male	T1D	23	96
38.5	male	T1D	32.5	73

In αiADKO mice, production of insulin-producing cells from α cells occurred without induction of embryonic islet regulators like *Neurog3*. In a prior study of Dox-induced Arx inactivation in mice (Courtney et al., 2013), lineage tracing reflected a schedule of constitutive Dox exposure and did not distinguish ductal cell from α cell progeny. In other work, continuous Arx inactivation from embryonic stages led to the development of polyhormonal cells (Wilcox et al., 2013). Future studies with complementary lineage-tracing methods would reinforce the findings and conclusions of our study.

scRNA-seq evaluation of converted α cells revealed rapid, extensive, and significant induction of gene expression networks known to regulate β cell fate and function, confirming our immunohistological findings (Arda et al., 2013; Maestro et al., 2007; Boj et al., 2010; Hunter et al., 2011) (Figure 5G). Our scRNA-seq analysis also revealed differences between these converted α cells and native β cells, reflecting the observed differences in hormone secretion. For example, only a subset of the converted α cells expressed β cell regulators like MafA, Pdx1, Nkx6.1, and Slc2a2. This heterogeneity of β cell gene expression within the population of converted α cells suggests that other β cell gene regulators may require activation to promote a more complete conversion toward a β cell fate.

Electrophysiological and hormone secretion assessments of cells undergoing α to β cell conversion confirmed our scRNA-seq predictions that a majority of the converted α cells are physiologically similar to normal β cells. We showed that Na^+ channel inactivation, a classical electrophysiological marker for distinguishing mouse α cells versus β cells, shifts from an α cell phenotype to a β cell phenotype in converted α cells. Moreover, we showed that converted α cells, like normal β cells, secrete insulin and show a clear switch to high-glucose amplification of exocytosis in contrast to unconverted α cells, which secrete glucagon and have exocytotic responses blunted by high glucose (Gylfe, 2016). We postulate that loss of *Arx* and *Dnmt1* in α cells triggers the upregulation of gene regulatory networks controlling metabolic sensing pathways that are intrinsic to β cells. Our findings suggest that additional extrinsic signaling modulation could additively enhance the pace and quality of α to β cell conversion achieved after targeted Arx and Dnmt1 inactivation. Thus, identifying signaling pathways that regulate Arx and Dnmt1 could be useful for directing α cells toward alternate fates.

Although mouse studies by us and others provide evidence that murine α cells can undergo conversion toward a β cell fate, the relevance of these findings to humans was unclear. Bi-hormonal human pancreatic cells, including glucagon$^+$ insulin$^+$ cells in subjects with diabetes (Piran et al., 2014; Yoneda et al., 2013) or in cultured islets (Bramswig et al., 2013), have been documented. However, the molecular or regulatory features underlying development of these abnormal glucagon$^+$ cells in T1D have not been described, reflecting inherent difficulties of pancreas procurement in humans with specific diseases. The finding of ARX and DNMT1 loss or reduction in glucagon$^+$ insulin$^+$ cells from two subjects with T1D corroborates prior studies in mice and human cell lines, suggesting that Arx or Dnmt1 establishes and/or maintains α cell fate and function (Collombat et al., 2003, 2007, 2009; Avrahami et al., 2015; Gage et al., 2015). Moreover, the abnormal expression of non-α cell factors, such as NKX6.1 and PDX1, in a subset of glucagon$^+$ cells is consistent with prior reports of impaired α cell function in T1D (Cryer et al., 2003; Pietropaolo, 2013). Here, we found glucagon$^+$ insulin$^+$ cells in the pancreata of two T1D donors less than 10 years of age with 4–5 years of disease, but not in three samples from older donors with a longer disease duration. The possibility that formation or maintenance of bi-hormonal glucagon$^+$ insulin$^+$ DNMT1^{Neg} cells in humans with T1D might depend on subject age, duration of disease, or other variables requires additional studies with more sampling. A previous study has reported the presence of residual insulin C-peptide in subjects with T1D of several decades' duration (Keenan et al., 2010). Because insulin or glucagon levels in our younger subjects are not known, the physiological relevance of these bi-hormonal cells remains unclear. Nevertheless, our findings suggest a potential molecular basis for compromised human α cell function in at least a subset of T1D patients. In summary, studies of human and mouse α cells here advance the understanding of α cell defects in T1D and promote the plausibility of targeted intra-islet cell conversion for regenerative goals.

EXPERIMENTAL PROCEDURES

Human Tissues

De-identified normal human pancreas specimens and pancreas specimens from type 1 diabetic donors were obtained from the International Institute for the Advancement of Medicine (IIAM) and the Network of Pancreatic Organ Donors (nPOD) (Table 1).

Mouse Studies

The *Glucagon-rtTA, Tet-o-Cre, R26-YFP* mouse has been described previously (Thorel et al., 2010). We generated four types of mice, all harboring the α cell lineage tracing system (Glucagon-rtTA, Tet-o-cre, R26-YFP): (1) control (with only the α cell lineage tracing system), (2) αiAKO (with the addition of floxed alleles to inactivate Arx, either $Arx^{f/Y}$ or $Arx^{f/f}$), (3) αiADKO (with the addition of floxed alleles to inactivate both Arx-$Arx^{f/Y}$ or $Arx^{f/f}$ and Dnmt1-$Dnmt1^{f/f}$), and (4) αiDKO (with addition of floxed alleles to inactivate Dnmt1-$Dnmt1^{f/f}$). To achieve lineage labeling and inactivation of Arx, Dnmt1, or both, DOX (Sigma) was administered via drinking water, which was prepared freshly every 2 days at 2 mg/mL for a total exposure of 3 weeks. After DOX removal, mice were maintained for an additional 4 or 12 weeks without DOX treatment before sacrifice. Glucagon-Venus mice, in which cells that express proglucagon are labeled by the YFP Venus, have been described previously (Reimann et al., 2008). All animal experiments and methods were approved by the Institutional Animal Care and Use Committee (IACUC) of Stanford University.

Immunohistology and Confocal Microscopy

Human pancreas sections were stained with antibodies against a panel of endocrine, as described previously (Chen et al., 2011). In brief, slides were

washed with PBS and blocked with normal donkey serum (5%), and primary antibodies were applied (Table S5). Antigen retrieval was performed for specified antibodies (Table S5) using antigen retrieval solution (S1699; DAKO) according to the manufacturer's instructions. Signal amplification using a biotin-streptavidin system (SP-2002; Vector Laboratories) and tyramide signal amplification (T30955; Thermo Fisher) were performed for specified antibodies (Table S5). For all mouse sections, in addition to the antibodies above, anti-YFP was used to detect YFP in lineage-marked α cells, and anti-Neurog3, Ki67, PPY, ghrelin, and Glut2 antibodies were used. Fluorescent secondary antibodies used were from Jackson ImmunoResearch or Molecular Probes (Table S6). Stained sections were mounted with VECTASHIELD Mounting Medium with DAPI (H-1200; Vector Laboratories) and visualized using a Leica SP2 inverted confocal laser scanning microscope (Supplemental Experimental Procedures).

Immuno-morphometry

For human sections, 60–100 islets were analyzed per staining and sample. Cells co-expressing GCG and a marker representative of another endocrine cell type were quantified as a percentage of the total number of GCG^+ cells counted. For mouse sections, islets were counted from four mice per genotype (Tables S1–S3). These analyses were non-randomized. The number of α cells undergoing conversion into other endocrine cell types (where "conversion" is defined as the expression of β, δ, or other endocrine cell genes in YFP^+ cells) was quantified as a percentage of total YFP^+ cells counted. Two-tailed Student's t test was used to determine whether the difference in the percentage of $Ki67^+$ YFP^+ cells between knockout and control mice was statistically significant ($p > 0.05$).

Statistical Analysis

Where indicated in the legends, graphed data in the figures are represented as mean ± SD for immuno-morphometry analyses.

Flow Cytometry

Isolated mouse islets were dissociated into single cells and processed as described (Supplemental Experimental Procedures). We collected cells from a YFP^+, lineage-traced population and a YFP^{Neg}, non-labeled population on a special-order five-laser FACS Aria II directly into a 96 well containing 4 μL lysis buffer with dNTPs[37] for downstream scRNA-seq assays.

scRNA-Seq and Data Analysis

scRNA-seq libraries were generated as described (Picelli et al., 2014). Briefly, single cells were lysed, followed by reverse transcription, pre-amplification, DNA purification, and analysis for successful amplification products. Barcoded sequencing libraries were prepared, and libraries were pooled and sequenced on the Illumina NextSeq instrument (Dobin and Gingeras, 2015; McKenna et al., 2010; Supplemental Experimental Procedures). Transcript counts were obtained using HT-Seq (Anders et al., 2015) and mm10 UCSC exon/transcript annotations. Pairwise distances between cells were estimated using Pearson correlation of overdispersed genes, as described (Fan et al., 2016). Subsequent hierarchical clustering was done using hclustfunction in R, and dimension reduction was performed using the tSNE method on pairwise distances (van der Maaten and Hinton, 2008). Data were also analyzed with QIAGEN IPA (www.ingenuity.com).

Electrophysiological Studies

Islets from control or αiADKO mice were dispersed to single cells and plated overnight on 35-mm dishes as described previously (Dai et al., 2011). Cells were patch clamped in the whole-cell voltage-clamp configuration, and Na^+ channels were activated by a depolarization to 0 mV following holding potentials ranging from −140 to 0 mV. Single-cell exocytosis was measured as described previously (Ferdaoussi et al., 2015). Briefly, cells were pre-incubated at either 2 or 20 mM glucose for 1 hr and transferred to a bath solution (Supplemental Experimental Procedures) with either 20 or 2 mM glucose ~10–30 min prior to patch clamping. Exocytosis was elicited by a series of ten 500-ms membrane depolarizations from −70 to 0 mV and monitored as increases in cell capacitance. Following the experiments, cells were immunostained for insulin and YFP to identify β cells (Ins^+ only), α cells (YFP^+ only), or converted α cells (Ins^+,YFP^+). Statistical analysis of exocytosis data was by two-way ANOVA, followed by Bonferroni post-test ($p < 0.05$ considered significant).

Hormone Secretion and Calcium Imaging

Hormone secretion and calcium imaging studies were performed as previously described (Adewola et al., 2010; Xing et al., 2016; Supplemental Experimental Procedures). Briefly, islets from MIP-GFP, glucagon-Venus, and αiADKO mice were dispersed into single cells, and GFP^+, $Venus^+$, or YFP^+ cells were collected by FACS as described above. For calcium imaging, the sorted cells were incubated in Kreb's ringer buffer (KRB) with 2 mM glucose and 5 μM Fura-2/AM (Molecular Probes) for 30 min, then loaded into a temperature-equilibrated microfluidic device mounted on an inverted epifluorescence microscope. KRB with 14 mM glucose or 2 mM glucose with 30 mM KCl was administered to the cells for 20 and 15 min, respectively. Dual-wavelength Fura-2/AM was excited at 340 and 380 nm (shift in excitation wavelength occurs upon binding Ca^{2+}), and fluorescent emission was detected at 510 nm. Intracellular Ca^{2+} concentration was expressed as a ratio of fluorescent emission intensity (percent of F340/F380). The fluorescence signal was expressed as a change in percentage after being normalized to basal intensity levels established before stimulation. For hormone secretion studies, 5,000 GFP^+ cells from MIP-GFP mice, $Venus^+$ cells from glucagon-Venus mice, or YFP^+ cells from αiADKO mice were collected by FACS and loaded onto the microfluidic device. To measure insulin secretion, YFP^+ cells were incubated in basal KRB with 2 mM glucose for 30 min and then stimulated with KRB containing 14 mM glucose for 30 min, followed by 2 mM glucose for 10 min. To measure glucagon secretion, YFP^+ cells were incubated in KRB with 11.2 mM glucose for 30 min and then stimulated with KRB with 2 mM glucose for 30 min. Ultrasensitive rodent insulin or glucagon ELISAs (Mercodia) were used to measure perfusate insulin or glucagon levels.

ACCESSION NUMBERS

The accession number for the scRNA-seq data reported in this paper is GEO: GSE79457.

SUPPLEMENTAL INFORMATION

Supplemental Information includes Supplemental Experimental Procedures, seven figures, and six tables and can be found with article online at http://dx.doi.org/10.1016/j.cmet.2017.01.009.

AUTHOR CONTRIBUTIONS

H.C. and N.D. performed the mouse and human pancreas studies with X.G. and C.D. J.W., X.G., and K.L. assisted H.C. with tissue collection and analysis from mice or humans. H.C., X.G., C.D., and N.D. performed immunohistochemistry and confocal microscopy. K.L. performed FACS analysis. M.E. and S.Q. performed and analyzed RNA-seq from sorted cells. S.C. performed IPA on the scRNA-seq data. X.D. and P.E.M. performed electrophysiological studies. Y.W., Y.X., and J.O. performed calcium imaging and hormone measures from dispersed cells. F.T., N.D., and P.L.H. generated mouse strains. H.C. and S.K.K. conceived the experiments, and H.C., P.L.H., and S.K.K. wrote the manuscript.

ACKNOWLEDGMENTS

We thank Dr. H.E. Arda for discussions for the FACS experiments; Dr. Y. Hang for help with islet isolations; members of the S.K.K. lab, especially Dr. S. Park, for advice; and Drs. J.A. Golden and L. Jackson-Grusby for the mouse strains. We also thank N. Neff and G. Mantalas for assistance with sequencing. H.C. was supported by a T32 training award to the Endocrinology Division, Department of Medicine, Stanford University School of Medicine, and fellowships from the Stanford Child Health Research Institute and the JDRF. C.D. was supported by Stanford University Vice-Provost Undergraduate Education grants. N.D. was supported by a grant from the Institute of Genetics and Genomics of Geneva. Effort in the S.Q. group was supported by NIH grants U01-HL099999 and U01-HL099995, California Institute of

Regenerative Medicine grant GC1R-06673, Center of Excellence for Stem Cell Genomics, The Wallenberg Foundation Postdoctoral Scholarship Program at Stanford, and the Howard Hughes Medical Institute (HHMI). The P.L.H. group was supported by grants from JDRF, the Swiss National Science Foundation, the NIH Beta Cell Biology Consortium (BCBC), and the European Union (IMIDIA), and the S.K.K. group was supported by HHMI, the H.L. Snyder Foundation, the Elser Trust, and grants from JDRF, the NIH BCBC (UO1DK089532 and UO1DK089572), and NIH Human Islet Resource Network (UC4DK104211).

Q1

Received: June 16, 2016
Revised: October 21, 2016
Accepted: January 17, 2017
Published: February 16, 2017

REFERENCES

Adewola, A.F., Lee, D., Harvat, T., Mohammed, J., Eddington, D.T., Oberholzer, J., and Wang, Y. (2010). Microfluidic perifusion and imaging device for multi-parametric islet function assessment. Biomed. Microdevices *12*, 409–417.

Akinci, E., Banga, A., Greder, L.V., Dutton, J.R., and Slack, J.M. (2012). Reprogramming of pancreatic exocrine cells towards a beta (β) cell character using Pdx1, Ngn3 and MafA. Biochem. J. *442*, 539–550.

Anders, S., Pyl, P.T., and Huber, W. (2015). HTSeq—a Python framework to work with high-throughput sequencing data. Bioinformatics *31*, 166–169.

Anderson, R.M., Bosch, J.A., Goll, M.G., Hesselson, D., Dong, P.D., Shin, D., Chi, N.C., Shin, C.H., Schlegel, A., Halpern, M., et al. (2009). Loss of Dnmt1 catalytic activity reveals multiple roles for DNA methylation during pancreas development and regeneration. Dev. Biol. *334*, 213–223.

Arda, H.E., Benitez, C.M., and Kim, S.K. (2013). Gene regulatory networks governing pancreas development. Dev. Cell *25*, 5–13.

Arda, H.E., Li, L., Tsai, J., Torre, E.A., Rosli, Y., Peiris, H., Spitale, R.C., Dai, C., Gu, X., Qu, K., et al. (2016). Age-dependent pancreatic gene regulation reveals mechanisms governing human β cell function. Cell Metab. *23*, 909–920.

Avrahami, D., Li, C., Zhang, J., Schug, J., Avrahami, R., Rao, S., Stadler, M.B., Burger, L., Schübeler, D., Glaser, B., et al. (2015). Aging-dependent demethylation of regulatory elements correlates with chromatin state and improved β cell function. Cell Metab. *22*, 619–632.

Benitez, C.M., Qu, K., Sugiyama, T., Pauerstein, P.T., Liu, Y., Tsai, J., Gu, X., Ghodasara, A., Arda, H.E., Zhang, J., et al. (2014). An integrated cell purification and genomics strategy reveals multiple regulators of pancreas development. PLoS Genet. *10*, e1004645.

Boj, S.F., Petrov, D., and Ferrer, J. (2010). Epistasis of transcriptomes reveals synergism between transcriptional activators Hnf1alpha and Hnf4alpha. PLoS Genet. *6*, e1000970.

Bramswig, N.C., Everett, L.J., Schug, J., Dorrell, C., Liu, C., Luo, Y., Streeter, P.R., Naji, A., Grompe, M., and Kaestner, K.H. (2013). Epigenomic plasticity enables human pancreatic α to β cell reprogramming. J. Clin. Invest. *123*, 1275–1284.

Chen, H., Gu, X., Liu, Y., Wang, J., Wirt, S.E., Bottino, R., Schorle, H., Sage, J., and Kim, S.K. (2011). PDGF signalling controls age-dependent proliferation in pancreatic β-cells. Nature *478*, 349–355.

Chera, S., Baronnier, D., Ghila, L., Cigliola, V., Jensen, J.N., Gu, G., Furuyama, K., Thorel, F., Gribble, F.M., Reimann, F., et al. (2014). Diabetes recovery by age-dependent conversion of pancreatic δ-cells into insulin producers. Nature *514*, 503–507.

Collombat, P., Mansouri, A., Hecksher-Sorensen, J., Serup, P., Krull, J., Gradwohl, G., and Gruss, P. (2003). Opposing actions of Arx and Pax4 in endocrine pancreas development. Genes Dev. *17*, 2591–2603.

Collombat, P., Hecksher-Sørensen, J., Krull, J., Berger, J., Riedel, D., Herrera, P.L., Serup, P., and Mansouri, A. (2007). Embryonic endocrine pancreas and mature beta cells acquire alpha and PP cell phenotypes upon Arx misexpression. J. Clin. Invest. *117*, 961–970.

Collombat, P., Xu, X., Ravassard, P., Sosa-Pineda, B., Dussaud, S., Billestrup, N., Madsen, O.D., Serup, P., Heimberg, H., and Mansouri, A. (2009). The ectopic expression of Pax4 in the mouse pancreas converts progenitor cells into alpha and subsequently beta cells. Cell *138*, 449–462.

Courtney, M., Gjernes, E., Druelle, N., Ravaud, C., Vieira, A., Ben-Othman, N., Pfeifer, A., Avolio, F., Leuckx, G., Lacas-Gervais, S., et al. (2013). The inactivation of Arx in pancreatic α-cells triggers their neogenesis and conversion into functional β-like cells. PLoS Genet. *9*, e1003934.

Cryer, P.E., Davis, S.N., and Shamoon, H. (2003). Hypoglycemia in diabetes. Diabetes Care *26*, 1902–1912.

Dai, X.Q., Plummer, G., Casimir, M., Kang, Y., Hajmrle, C., Gaisano, H.Y., Manning Fox, J.E., and MacDonald, P.E. (2011). SUMOylation regulates insulin exocytosis downstream of secretory granule docking in rodents and humans. Diabetes *60*, 838–847.

Dai, X.Q., Spigelman, A.F., Khan, S., Braun, M., Manning Fox, J.E., and MacDonald, P.E. (2014). SUMO1 enhances cAMP-dependent exocytosis and glucagon secretion from pancreatic α-cells. J. Physiol. *592*, 3715–3726.

Dhawan, S., Georgia, S., Tschen, S.I., Fan, G., and Bhushan, A. (2011). Pancreatic β cell identity is maintained by DNA methylation-mediated repression of Arx. Dev. Cell *20*, 419–429.

Dhawan, S., Tschen, S.I., Zeng, C., Guo, T., Hebrok, M., Matveyenko, A., and Bhushan, A. (2015). DNA methylation directs functional maturation of pancreatic β cells. J. Clin. Invest. *125*, 2851–2860.

Dobin, A., and Gingeras, T.R. (2015). Mapping RNA-seq reads with STAR. Curr. Protoc. Bioinformatics *51*, 1–19.

Efe, J.A., Hilcove, S., Kim, J., Zhou, H., Ouyang, K., Wang, G., Chen, J., and Ding, S. (2011). Conversion of mouse fibroblasts into cardiomyocytes using a direct reprogramming strategy. Nat. Cell Biol. *13*, 215–222.

Fan, J., Salathia, N., Liu, R., Kaeser, G.E., Yung, Y.C., Herman, J.L., Kaper, F., Fan, J.B., Zhang, K., Chun, J., et al. (2016). Characterizing transcriptional heterogeneity through pathway and gene set overdispersion analysis. Nat. Methods *13*, 241–244.

Ferdaoussi, M., Dai, X., Jensen, M.V., Wang, R., Peterson, B.S., Huang, C., Ilkayeva, O., Smith, N., Miller, N., Hajmrle, C., et al. (2015). Isocitrate-to-SENP1 signaling amplifies insulin secretion and rescues dysfunctional β cells. J. Clin. Invest. *125*, 3847–3860.

Fulp, C.T., Cho, G., Marsh, E.D., Nasrallah, I.M., Labosky, P.A., and Golden, J.A. (2008). Identification of Arx transcriptional targets in the developing basal forebrain. Hum. Mol. Genet. *17*, 3740–3760.

Gage, B.K., Asadi, A., Baker, R.K., Webber, T.D., Wang, R., Itoh, M., Hayashi, M., Miyata, R., Akashi, T., and Kieffer, T.J. (2015). The role of ARX in human pancreatic endocrine specification. PLoS ONE *10*, e0144100.

Göpel, S.O., Kanno, T., Barg, S., Weng, X.G., Gromada, J., and Rorsman, P. (2000). Regulation of glucagon release in mouse -cells by KATP channels and inactivation of TTX-sensitive Na^+ channels. J. Physiol. *528*, 509–520.

Gradwohl, G., Dierich, A., LeMeur, M., and Guillemot, F. (2000). neurogenin3 is required for the development of the four endocrine cell lineages of the pancreas. Proc. Natl. Acad. Sci. USA *97*, 1607–1611.

Gu, G., Dubauskaite, J., and Melton, D.A. (2002). Direct evidence for the pancreatic lineage: $NGN3^+$ cells are islet progenitors and are distinct from duct progenitors. Development *129*, 2447–2457.

Gylfe, E. (2016). Glucose control of glucagon secretion—'There's a brand-new gimmick every year'. Ups. J. Med. Sci. *121*, 120–132.

Hunter, C.S., Maestro, M.A., Raum, J.C., Guo, M., Thompson, F.H., 3rd, Ferrer, J., and Stein, R. (2011). Hnf1α (MODY3) regulates β-cell-enriched MafA transcription factor expression. Mol. Endocrinol. *25*, 339–347.

Itoh, M., Takizawa, Y., Hanai, S., Okazaki, S., Miyata, R., Inoue, T., Akashi, T., Hayashi, M., and Goto, Y. (2010). Partial loss of pancreas endocrine and exocrine cells of human ARX-null mutation: consideration of pancreas differentiation. Differentiation *80*, 118–122.

Keenan, H.A., Sun, J.K., Levine, J., Doria, A., Aiello, L.P., Eisenbarth, G., Bonner-Weir, S., and King, G.L. (2010). Residual insulin production and pancreatic ß-cell turnover after 50 years of diabetes: Joslin Medalist Study. Diabetes *59*, 2846–2853.

Kim, S.K., Baldwin, K., Gao, S., Bücker, C., Parmar, M., and Benvenisty, N. (2016). iPSCs: 10 years and counting. Cell *165*, 1041–1042.

Kordowich, S., Collombat, P., Mansouri, A., and Serup, P. (2011). Arx and Nkx2.2 compound deficiency redirects pancreatic alpha- and beta-cell differentiation to a somatostatin/ghrelin co-expressing cell lineage. BMC Dev. Biol. *11*, 52.

Maestro, M.A., Cardalda, C., Boj, S.F., Luco, R.F., Servitja, J.M., and Ferrer, J. (2007). Distinct roles of HNF1beta, HNF1alpha, and HNF4alpha in regulating pancreas development, beta-cell function and growth. Endocr. Dev. *12*, 33–45.

Mastracci, T.L., Wilcox, C.L., Arnes, L., Panea, C., Golden, J.A., May, C.L., and Sussel, L. (2011). Nkx2.2 and Arx genetically interact to regulate pancreatic endocrine cell development and endocrine hormone expression. Dev. Biol. *359*, 1–11.

McKenna, A., Hanna, M., Banks, E., Sivachenko, A., Cibulskis, K., Kernytsky, A., Garimella, K., Altshuler, D., Gabriel, S., Daly, M., et al. (2010). The Genome Analysis Toolkit: a MapReduce framework for analyzing next-generation DNA sequencing data. Genome Res. *20*, 1297–1303.

Morán, I., Akerman, I., van de Bunt, M., Xie, R., Benazra, M., Nammo, T., Arnes, L., Nakić, N., García-Hurtado, J., Rodríguez-Seguí, S., et al. (2012). Human β cell transcriptome analysis uncovers lncRNAs that are tissue-specific, dynamically regulated, and abnormally expressed in type 2 diabetes. Cell Metab. *16*, 435–448.

Morris, S.A., and Daley, G.Q. (2013). A blueprint for engineering cell fate: current technologies to reprogram cell identity. Cell Res. *23*, 33–48.

Papizan, J.B., Singer, R.A., Tschen, S.I., Dhawan, S., Friel, J.M., Hipkens, S.B., Magnuson, M.A., Bhushan, A., and Sussel, L. (2011). Nkx2.2 repressor complex regulates islet β-cell specification and prevents β-to-α-cell reprogramming. Genes Dev. *25*, 2291–2305.

Park, J.H., Stoffers, D.A., Nicholls, R.D., and Simmons, R.A. (2008). Development of type 2 diabetes following intrauterine growth retardation in rats is associated with progressive epigenetic silencing of Pdx1. J. Clin. Invest. *118*, 2316–2324.

Picelli, S., Faridani, O.R., Björklund, A.K., Winberg, G., Sagasser, S., and Sandberg, R. (2014). Full-length RNA-seq from single cells using Smart-seq2. Nat. Protoc. *9*, 171–181.

Pietropaolo, M. (2013). Persistent C-peptide: what does it mean? Curr. Opin. Endocrinol. Diabetes Obes. *20*, 279–284.

Piran, R., Lee, S.H., Li, C.R., Charbono, A., Bradley, L.M., and Levine, F. (2014). Pharmacological induction of pancreatic islet cell transdifferentiation: relevance to type I diabetes. Cell Death Dis. *5*, e1357.

Reimann, F., Habib, A.M., Tolhurst, G., Parker, H.E., Rogers, G.J., and Gribble, F.M. (2008). Glucose sensing in L cells: a primary cell study. Cell Metab. *8*, 532–539.

Schaffer, A.E., Taylor, B.L., Benthuysen, J.R., Liu, J., Thorel, F., Yuan, W., Jiao, Y., Kaestner, K.H., Herrera, P.L., Magnuson, M.A., et al. (2013). Nkx6.1 controls a gene regulatory network required for establishing and maintaining pancreatic beta cell identity. PLoS Genet. *9*, e1003274.

Shu, J., Wu, C., Wu, Y., Li, Z., Shao, S., Zhao, W., Tang, X., Yang, H., Shen, L., Zuo, X., et al. (2013). Induction of pluripotency in mouse somatic cells with lineage specifiers. Cell *153*, 963–975.

Thorel, F., Népote, V., Avril, I., Kohno, K., Desgraz, R., Chera, S., and Herrera, P.L. (2010). Conversion of adult pancreatic alpha-cells to beta-cells after extreme beta-cell loss. Nature *464*, 1149–1154.

van der Maaten, L., and Hinton, G. (2008). Visualizing data using t-SNE. J. Mach. Learn. Res. *9*, 2579–2605.

Wilcox, C.L., Terry, N.A., Walp, E.R., Lee, R.A., and May, C.L. (2013). Pancreatic α-cell specific deletion of mouse Arx leads to α-cell identity loss. PLoS ONE *8*, e66214.

Xing, Y., Nourmohammadzadeh, M., Elias, J.E., Chan, M., Chen, Z., McGarrigle, J.J., Oberholzer, J., and Wang, Y. (2016). A pumpless microfluidic device driven by surface tension for pancreatic islet analysis. Biomed. Microdevices *18*, 80.

Yang, Y.P., Thorel, F., Boyer, D.F., Herrera, P.L., and Wright, C.V. (2011). Context-specific α- to-β-cell reprogramming by forced Pdx1 expression. Genes Dev. *25*, 1680–1685.

Yoneda, S., Uno, S., Iwahashi, H., Fujita, Y., Yoshikawa, A., Kozawa, J., Okita, K., Takiuchi, D., Eguchi, H., Nagano, H., et al. (2013). Predominance of β-cell neogenesis rather than replication in humans with an impaired glucose tolerance and newly diagnosed diabetes. J. Clin. Endocrinol. Metab. *98*, 2053–2061.